Available online at www.sciencedirect.com
ScienceDirect
Composites Science and Technology 68 (2008) 1258–1265
COMPOSITES SCIENCE AND TECHNOLOGY
www.elsevier.com/locate/compscitech

Analysis of damage mechanisms and associated acoustic emission in two SiC_f/[Si–B–C] composites exhibiting different tensile behaviours. Part II: Unsupervised acoustic emission data clustering

M. Moevus, N. Godin *, M. R'Mili, D. Rouby, P. Reynaud, G. Fantozzi, G. Farizy

MATEIS, INSA-Lyon, 7 Avenue Jean Capelle, 69621 Villeurbanne, France

Received 5 July 2007; received in revised form 16 November 2007; accepted 2 December 2007
Available online 30 January 2008

Abstract

The present work deals with two SiC_f/[Si–B–C] composites exhibiting very different mechanical behaviours under tensile testing: low strain to failure for the one, high strain to failure for the other with similar ultimate strength. In the present Part II, emphasis is made on the clustering procedure of the recorded acoustic emission data. Clustering results are discussed as regards of what is known about the damage mechanisms operating in both composites (see Part I of this work [Moevus M, Rouby D, Godin N, R'Mili M, Reynaud P, Fantozzi G, et al. Analysis of damage mechanisms and associated acoustic emission in two SiC/[Si–B–C] composites exhibiting different tensile curves. Part I: Damage patterns and acoustic emission activity. Compos Sci Technol; in press]) [1]. The different types of matrix cracking in the composite are successfully distinguished by the AE analysis. This methodology will further be applied to static fatigue tests at intermediate temperature, in order to help predicting lifetimes of the composite.

Keywords: A. Ceramic matrix composites; D. Acoustic emission; C. Data clustering; C. *k*-means method

1. Introduction

An experimental study of two SiC_f/[Si–B–C] composites exhibiting different behaviours has been presented in a companion paper [1]. The difference in the mechanical behaviours has been attributed to a difference in the interfacial shear stress. The global acoustic emission (AE) activity and the microscopic observations of both composites have been compared in order to highlight the differences in damage accumulation. This second part deals more precisely with a statistical multi-variate analysis of the AE data, in order to distinguish the signals produced by the different damage mechanisms.

Acoustic emission is a transient wave resulting from the sudden release of stored energy during a damage process [2–4]. These waves propagate through the specimen and are transformed in electrical signals by piezoelectric transducers. The signals depend on the AE source, the propagation medium and the sensors, thus there is no universal signature of damaging events. However in permanent set-up conditions similarities exist among AE signals originating from similar events. In this way a careful analysis of the AE signals can lead to the discrimination of the different damage mechanisms occurring in a composite (matrix cracking, fibre breaks, interfacial debonding, frictional sliding). Most studies have used AE descriptors such as amplitude or duration to characterize the AE sources. A single parameter analysis is sometimes sufficient to discriminate two mechanisms with very different energies. Some authors applied this type of analysis to CMCs [5–7]. In the case of CMCs, Morscher used the energy of the waveforms to correlate through thickness matrix cracks, considering that the signals of fibre failure and interfacial debonding and sliding have a negligible contribution in energy [8,9]. However, a discrimination of the acoustic signatures of the damage

* Corresponding author. Tel.: +33 472 438 073; fax: +33 472 438 528.
E-mail address: nathalie.godin@insa-lyon.fr (N. Godin).

0266-3538/$ - see front matter © 2007 Elsevier Ltd. All rights reserved.
doi:10.1016/j.compscitech.2007.12.002

mechanisms based only on one parameter is debatable in such composites, because the amplitude distribution is generally not clearly multimodal. A multi-variate analysis using statistical pattern recognition techniques is more appropriate and can give interesting results [10–18].

An alternative to parametric analysis is transient analysis: all the waveforms are digitized and analysed. Interesting works have been carried out on the frequency content of the signals in order to differentiate the different propagation modes and the damage mechanisms [19–22]. In the present study the large amount of AE data was dissuasive, because transient analysis needs extensive acquisition and storage capacities, and is very time demanding for analysing each waveform. A statistical multi-variate data analysis was preferred. Its efficiency to identify damage mechanism has been proven by several authors for some ceramic matrix composites [12–14].

The chosen AE clustering methodology has been described elsewhere [23] but some improvements have been made. The entire procedure is described in Section 2. Particular care was taken in order to optimize the AE data description before clustering. This methodology was applied to the data obtained during mechanical testing of two SiC_f/[Si–B–C] composites with different mechanical behaviours. The damage accumulation of both composites has been analysed and compared in [1]. The experimental procedure will be briefly recalled in Section 3. Afterwards Section 4 gives a rapid description of the damage accumulation. Next the clustering results are presented and compared in Section 5. Lastly the clusters will be associated with damage mechanisms in Section 6.

2. Unsupervised clustering methodology of the AE signals

In this work the AE signals will be treated as pattern vectors described by a number d of features, or descriptors (amplitude, duration, rise time, counts, etc.). The number d is the dimensionality of the pattern vector. As defined by Jain et al. [24,25] clustering refers to unsupervised classification. No labelled data is available in our case, thus an unsupervised methodology is required to perform an exploratory pattern-analysis. A typical pattern clustering involves the following steps:

- representation of the pattern vectors (feature selection/extraction procedure),
- definition of a similarity measure appropriate to the data domain,
- clustering (or grouping of similar pattern vectors),
- cluster validity analysis (using a specific criterion of optimality),
- labelling the clusters (identifying the AE sources).

Each step will be described in this section (except labelling which will be discussed in Section 6). All the procedure is unsupervised and aims at extracting the natural structure of the data. Particular care was taken for the pattern representation since it determines the final output of the clustering: with too many redundant features it is possible to make two arbitrary patterns similar.

2.1. Feature selection using hierarchical clustering

This step is based on the methodology used by Anastassopoulos et al. [10,11] for feature selection. The AE data was initially described by 18 features given in Fig. 1. The 9 first ones (like the rise time R or the amplitude A) are calculated by the acquisition system, the others are ratios of the first ones (for example: R/A). Notice that the average frequency is in fact an apparent frequency equal to the number of counts divided by the duration of the signal. The further calculation of correlation coefficients implies the assumption that all the AE features exhibit Gaussian-like distributions. This was clearly not the case for several features such as the duration D or the energy E, which exhibit exponential distributions. Thus the logarithmic values of such descriptors (noted $D_{\ln}$, $E_{\ln}$) were used instead of their natural values. The feature values were then normalized in the range $[-1.0; 1.0]$ in order to obtain comparable scales between all the descriptors.

The correlation matrix of the 18 features was calculated and subjected to a complete link hierarchical clustering [26]. This clustering aims at merging the correlated features into groups, the correlation matrix being updated after each grouping of two features. The result can be plotted in a dendrogram (Fig. 1). The determination of a threshold fixes the number of groups to be considered. It was chosen so as to select a subset of eight features. With more than eight features, the final result of the clustering procedure remains the same, so the other features are redundant. The selected features are circled in the list of Fig. 1.

2.2. Feature extraction using a principal component analysis (PCA)

A principal component analysis was performed in order to define new uncorrelated features and to reduce the dimensionality of the data [27,28]. The correlation matrix R of the eight features is calculated. The eigenvectors and their associated eigenvalues are extracted. The eigenvectors V_i are linear combinations of the eight features mentioned below:

$$V_i = a_i R_{\ln} + b_i F + c_i RF + d_i E_{\ln} + e_i R/D_{\ln} + f_i A/R_{\ln} + g_i A/DT_{\ln} + h_i A/F_{\ln}, \quad (1)$$

where $a_i, b_i \ldots, h_i$ are constants, and $R_{\ln}$, F, RF, $E_{\ln}$, $R/D_{\ln}$, $A/R_{\ln}$, $A/DT_{\ln}$, $A/F_{\ln}$ are the selected features from the dendrogram (see Fig. 1). They have the particularity of being uncorrelated, so the initial eight-dimensional domain of data's description is transformed in an orthogonal one, and the eigenvectors form the new base of this domain. The eigenvectors correspond to the dimensions with the largest variances. The exact contribution of the kst eigenvector to

(1)	log(Rise time)	R_{ln}
2	log(Counts)	C_{ln}
3	log(Duration)	D_{ln}
4	Amplitude	A
(5)	average Frequency	F
6	Counts to Peak	CP
7	Decay Frequency	DF
(8)	Rise Frequency	RF
(9)	log(Energy)	E_{ln}
(10)	log(Rise time/Duration)	R/D_{ln}
11	log(Duration/Amplitude)	D/A_{ln}
12	log(Decay Time)	DT_{ln}
(13)	log(Ampl./Rise time)	A/R_{ln}
(14)	log(Ampl./Decay Time)	A/DT_{ln}
15	log(rise/Decay Time)	R/DT_{ln}
16	log(Energy/Amplitude)	E/A_{ln}
17	Counts to Peak/Counts	P/C
(18)	log(Ampl./avg Freq.)	A/F_{ln}

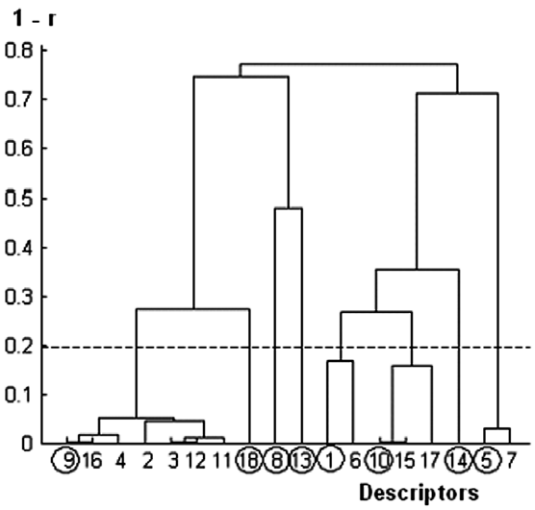

Fig. 1. Correlation dendrogram of the AE descriptors.

the total variance of the data is given by the ratio $\lambda_k/(\lambda_1+\lambda_2+\cdots+\lambda_8)$ where λ_k is the kst eigenvalue associated with the kst eigenvector. Therefore the principal components are the j most representative eigenvectors. In this work, j was defined as the minimum number of eigenvalues that contribute to more than 95% of the variance of the data by summing their contributions, and j was found equal to 4. The other eigenvectors can be neglected without loosing much information. Finally the data was expressed in the four-principal components' base.

Johnson [18] applied the PCA as an unsupervised clustering method for the AE data generated during tensile tests on glass fibre/epoxy laminates. Two principal components have been identified, which allow the visualization of the data in a two-axis graph. Clusters could immediately be identified. In the present work, with four-principal components the visualization of clusters is not obvious and the use of an unsupervised clustering algorithm is necessary.

2.3. Similarity measure: a weighted Euclidean distance

In order to take into account that the principal components do not contain the same quantity of information, the distance between two points in this 4D-space is defined as $d_w^2(X,Y)=\sum_{i=1}^{4}\lambda_i.(X_i-Y_i)^2$ where λ_i is the ist eigenvalue, X_i and Y_i are the ist coordinates of the vectors X and Y. The distance d_w^2 is a squared weighted Euclidean distance. It will be used in all the following steps.

2.4. Clustering by the k-means algorithm

The k-means algorithm aims at minimizing the sum of squared distances between all the vectors of a cluster and its centre [29]. This method assumes that the number k of clusters is specified in advance. The coordinates of the cluster centres are randomly initialized. Then each pattern is assigned to the nearest cluster, according to the weighted Euclidean distance between the pattern and the centres of the clusters. Afterwards the new coordinates of the centres are computed and the procedure is repeated until there is no change in the coordinates of the centres. The main problem is that this algorithm can reach either a local or global convergence depending on the initialisation. To avoid this difficulty, a random uniform initialization was chosen rather than a simple random one. This leads to a more reproducible result. Moreover the clustering was run 15 times and only the best result was saved.

2.5. Cluster validity: Davies and Bouldin criterion

The optimal number of clusters k was empirically determined by using the Davies and Bouldin criterion [30], which does not depend on k. The Davies and Bouldin coefficient DB is defined as $\mathrm{DB}=\frac{1}{k}\sum_{i=1}^{k}\max_{i\neq j}\left\{\frac{d_i+d_j}{D_{ij}}\right\}$ where d_i and d_j are the average within-class distances of clusters i and j respectively, and D_{ij} denotes the distance between the two clusters i and j. The best clustering result corresponds to a minimum value of DB. So several clusterings were performed with k varying from 2 to 10, and the optimal number k was chosen so as to minimize DB.

3. Experimental procedure

The materials and mechanical tests monitored by AE have been described in [1]. They will be briefly recalled. The studied materials are SiC_f/[Si–B–C] composites exhibiting very different mechanical behaviours because of a different interfacial shear stress. The composite having a larger strain to failure is called M–E ("Elongation"), and the other M–S ("Stiffness"). One specimen of each material was tested at room temperature. The specimens were loaded in tension up to a specific load value corresponding to a strain equal to 0.3%. The load was hold during nearly 20 h. Unloading cycles were applied before performing a residual tensile test up to failure. AE was monitored by

using a two-channel MISTRAS 2001 acquisition system of Physical Acoustics Corporation. Two resonant MICRO-80 sensors were attached on the specimen 78 mm apart. Medium viscosity vacuum grease was used as a coupling agent. The acquisition parameters were set as follows: threshold 40 dB, peak definition time 50 μs, hit definition time 100 μs, hit lockout time 1000 μs. The location procedure and AE filtering have been described in [1].

4. Damage description and expectations for the AE clustering

In such CMCs, matrix cracking can be classified into several kinds of cracking. First, cracks initiate in the external seal-coat and at the macropores inside the composite, and propagate through the inter-yarn matrix (C1). Then the cracks propagate inside the transverse yarns through fibre–matrix interfaces (C2). Multiple matrix cracking finally occurs inside the axial yarns (C3). These cracks are deflected by the fibre–matrix interphase layer (C4), leading to fibre debonding and overloading. Some fibre breaks are expected under high stresses. They rapidly lead to instable fracture of entire yarns and of the composite.

Microscopic observations after failure revealed that the crack networks of M–E and M–S are rather different [1]. M–S contains much more cracks than M–E, so the mean crack spacing values (and pull-out lengths) are smaller in M–S (Table 1 in [1]). The crack spacing measurements also confirm the observation that matrix cracking saturation in the axial yarns is reached in M–E at the end of the test, but not in M–S. Moreover a dense cracking was observed in a particular matrix layer of M–S (C5) which was not visible in M–E.

According to these observations some expectations can be formulated on the corresponding AE. The sources of AE are the different matrix cracks, interfacial debonding, individual fibre fractures and yarn fractures. After clustering of the AE data, the maximum possible number of clusters may be equal to the number of mechanisms if all the acoustic signatures are distinguishable. But some mechanisms may produce similar AE signals that would not be separated by the clustering algorithm. In this case the number of clusters would be less than the number of mechanisms. The energy of the AE signals is related to the energy released by the AE source. This parameter is thus very important to discriminate the different mechanisms. It depends on the size of the source, on the material strength and on the stored elastic energy.

Three types of matrix cracking (C1, C2, C3) have been observed in both composites [1] which can produce three types of signals, because they have different morphologies and sizes (Table 1): C1-cracks cross several matrix layers (~0.2 mm length) and several yarns (their width is several millimetres according to microscopic observations); C2-cracks inside the transverse yarns are parallel to the fibres and travel through matrix layers and interphases. Therefore these cracks may propagate step by step. Their length is limited by the yarn's thickness (0.1–0.2 mm) and their width could be approximately 3 mm (distance between two crossed axial yarns → zones in compression) but it was not possible to really measure the size of such cracks; C3-cracks inside the axial yarns are the shortest ones because their area is limited by the cross-sectional area of one yarn (approximately 1 mm width and 0.1–0.2 mm thick).

One additional type of cracking (C5) has been observed in M–S which should lead to an additional cluster of signals in M–S: the width of such cracks is similar to that of C1-cracks but their length is limited by the layer's thickness (~0.05 mm). So the corresponding AE signals may have a smaller energy than those associated with C1-cracks but a higher energy than those associated with C3-cracks.

Debonding in the axial yarns (C4) is consecutive to C3-cracks in the axial yarns. This mechanism should produce low energy signals since debonding is limited by both the fibre perimeter (0.05 mm) and the debonding length (~0.3 mm in M–E and 0.05 mm in M–S).

Before the final fracture of the composite, some fibre breaks may be recorded. When the consecutive overloading on the survival fibres is too high, entire yarns fail leading to the fracture of the specimen. These last signals may have a higher energy than the individual fibre breaks. We have no *a priori* information about the energy of fibre breaks signals in comparison with the energy of matrix

Table 1
List and characteristics of the AE sources and clusters of signals

AE source		C1-cracks	C2-cracks	C3-cracks	C4-debonding	C5-cracks	Fibre fracture	Yarn fracture
Crack area (mm^2)	M–E	0.4–0.8	0.3–0.6	0.1–0.2	0.015	–	0.00015	0.1–0.2
	M–S				0.003	0.15–0.25		
Number of cracks	M–E	1500–3000	3000	25000	?	–	–	–
	M–S	3000–8000	5000	150000	?	6000–16000	–	–
AE cluster		A	B	C (+F)	D	E		
Energy (attoJ)	M–E	118440	2220	260	200	–		
	M–S	152800	2710	170	205	850		
Number of events	M–E	2396	5560	3676	2784	–		
	M–S	7246	9686	11900	4484	8172		

cracks because it depends both on the fracture area, the Young's modulus of the constituents and their strain to failure. Therefore the comparison between the energy released by matrix cracking and by fibre fracture is not obvious.

In the case of matrix cracking, rough estimations of the number of cracks can be made by considering the presence of approximately 16 axial yarns in the width of the specimen, nine rows in the thickness in M–E and 12 rows in M–S, and a monitored specimen's length of 60 mm. The crack spacing distances were measured for each type of cracks in [1]. All the possible AE sources, their characteristics and expected number of events are summarized in Table 1.

5. AE data clustering results

The AE clustering procedure described in Section 2 has been applied to the AE data recorded during the previously described tests on M–E and M–S. The signals recorded during the unload–reload cycles have been suppressed because they are very few, and in the case of M–E they are principally produced by interfacial sliding which is not considered as a damage mechanism.

5.1. Description of the obtained clusters

According to the Davies and Bouldin criterion, the optimal clustering was obtained with four clusters in M–E and with six clusters in M–S. This corresponds to the minimum values of Davies and Bouldin coefficient as shown in Fig. 2. Table 2 summarizes the mean characteristics of the obtained clusters of AE signals. The A, B, C, D clusters of M–E, ranked by energy, are also present in M–S and have the same mean characteristics. Two additional clusters E and F appeared in M–S. A-type signals are the biggest ones: highest energy, duration and amplitude. B-type signals can be distinguished by lower energy, higher rise time to duration ratio and higher apparent frequency than the cluster A. Clusters C and D exhibit quite the same low energy but C presents the shortest rise time whereas D has the longest one, the corresponding waveforms are thus really different. In M–S composite, cluster E appears intermediate between B and C; it differs from B by its very short rise time and from C by its high frequency. Cluster F has a very short duration but its rise time and rise frequency are similar to those of cluster C. For the low amplitude signals (C, D and F) the acquisition threshold has a strong influence on the AE descriptors calculation, and particularly on the duration of the signals. The decay part of the waveform may be shortened because the ultimate counts of the waveform may be lower than the threshold value. Therefore, since only the decay characteristics of the F-type signals differ from the C-ones, the cluster F seems to be a part of cluster C, which has been separated by the algorithm in the case of M–S because of the very large number of signals in this composite. In the following we consider that C- and F-type signals belong to the same cluster (C + F).

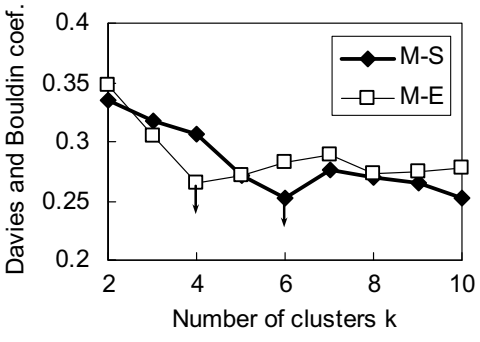

Fig. 2. Davies and Bouldin criterion: the minimum values of coefficient DB are obtained with four clusters in M–E and six clusters in M–S.

5.2. The AE activity associated with each cluster

The clusters' activities are shown in Fig. 3 for both materials. The proper activities of the different clusters are not very far from the global activity as described in [1]. Nevertheless some differences can be noticed. In the case of M–E (Fig. 3a), cluster B is the most active from the beginning of the test, before yielding, and its activity increases during the residual tensile test. The same feature is observed for the clusters A and C, but these clusters are less active during the load hold sequence and seem to saturate. Conversely the cluster D is less active during the initial loading and its activity increases during the other steps. In M–S (Fig. 3b) the trend is overall similar except that the clusters A and (C + F) are more active. Here, the cluster E is one of the most active and cannot be neglected. All the clusters exhibit significant activity during the load hold step. We notice that C is inactive at the end of the test in M–E, and that this is not the case for (C + F) in M–S. The main information about the clusters is summarized in Table 1: energy and number of events in each composite.

The residual tensile test leads to final fracture. It is shown in [1] that there is a local concentration of the AE events in the fracture zone before the final fracture of M–E. It is thus interesting to analyse which cluster is more linked with what happens during fracture. To do this, the signals coming from the fracture zone (in the interval of position [+12;+22] mm in M–E, [+8;+18] mm in M–S, 0 being the gauge length centre) are separated from the rest of the data. Concerning the so-called unbroken zone, the number of events is averaged in order to give the number of AE events for the same zone length as the fracture zone one (10 mm). The M–E clusters' activities in the unbroken zone and in the fracture zone are compared in Fig. 4. It appears very clearly that clusters A and B rise more steeply in the fracture zone before fracture than in the other zone. Clusters A and B also manifestly increase in the fracture zone for M–S material.

Table 2
Mean characteristics of the clusters

	Cluster	Energy (attoJ)	Amplitude (dB)	Risetime (μs)	Duration (μs)	Risetime/duration	Frequency (kHz)
M–E	A	118440	83	10	852	0.01	210
	B	2220	65	12	168	0.07	264
	C	260	57	4	73	0.05	180
	D	200	55	23	76	0.31	165
M–S	A	152840	83	9	1057	0.01	215
	B	2710	65	14	206	0.07	237
	C	180	55	5	76	0.07	128
	D	200	54	28	86	0.32	142
	E	850	62	3	117	0.03	224
	F	140	54	9	38	0.24	247

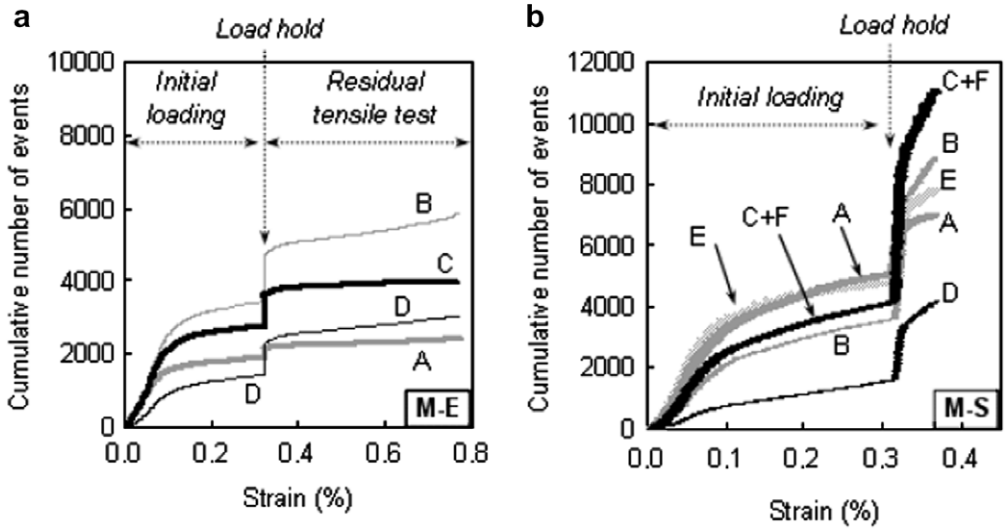

Fig. 3. Activities of the clusters during the test, (a) in M–E and (b) in M–S composite.

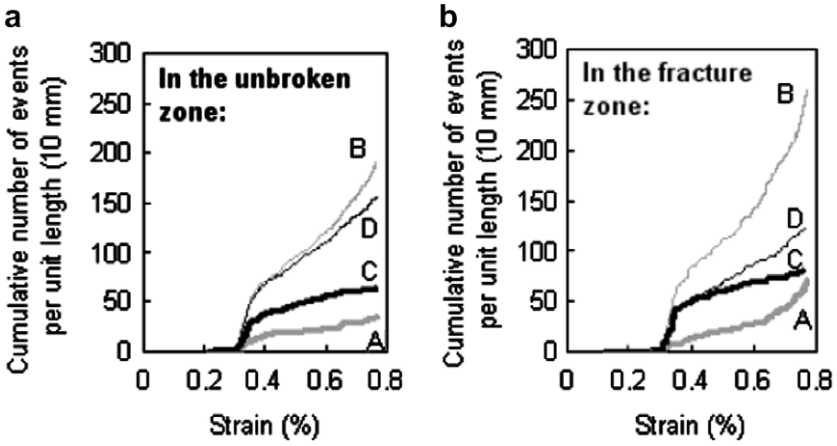

Fig. 4. Comparison of the clusters' activities (a) in the unbroken zone and (b) in the fracture zone, during the residual tensile test on M–E composite.

6. Discussion

The results are in good agreement with what was expected after damage descriptions (Section 4). All the clusters found in M–E are also present in M–S with very similar characteristics; in the same way, all the mechanisms occurring in M–E also occur in M–S. Moreover two additional clusters were isolated in M–S, in which one additional mechanism has been observed. It has been shown that the second additional cluster could be joined to another one because their main characteristics are similar. Therefore the preceding results of unsupervised clustering

allow the proposition of an identification of damage mechanisms associated with clusters of signals. The discussion will be organised in five paragraphs, each one corresponding to one cluster. The identification with one or more mechanisms (described in Table 1) will be discussed taking into account the mean characteristics of the cluster (and particularly the energy level of the signals), its activity in link with the applied loadings, and the expected number of signals.

Cluster A appears in great majority at the beginning of the test, during initial loading (Fig. 3), so it should correspond to some matrix cracking. Since this cluster groups the signals having the highest energy level (Table 1), it is associated with C1-cracks, which are the biggest observed cracks. The number of A-type signals is in good agreement with the number of C1-cracks in M–E and in M–S composites (Table 1). This mechanism is expected to saturate, but in reality some activity is recorded during the residual tensile test just before failure in the failure zone (Fig. 4). This suggests that this cluster also contains fracture signals associated with the final fracture of the composite. These signals are attributed to some yarn's fracture or collective fibre breaks (individual fibre failures will rather be associated to cluster B of lower energy). As a conclusion, the cluster A contains signals from two damage mechanisms which are chronologically well separated. It is thus possible to refine the clustering result by extracting the last fracture signals from cluster A.

Cluster B is also active from the beginning of initial loading, we thus associate it with another type of matrix cracking. These signals have the second place according to the energy rank (Table 1), so they can be attributed to C2-cracks. By comparing the number of C2-cracks and the number of B-type signals, it appears that there are two or three times more signals than cracks. However the estimation of the number of cracks is not precise at all because the cracks' width could not be measured. Moreover, the C2-cracks propagate step by step through matrix layers and interphase layers around the transverse fibres, and can produce several AE signals per crack. This cluster has a significant activity during the load hold step (Fig. 3). It is coherent because under constant load a propagation of debonding at the fibre–matrix interfaces is expected. This debonding occurs both in transverse yarns (C2-cracks) and in axial yarns. According to Fig. 4, cluster B is also linked with the final fracture of the composite, since its activity locally increases in the fracture zone just before failure. These last signals can thus be associated with fibre breaks. It seems difficult for the clustering algorithm to isolate the fibre fractures from the rest of the AE data, certainly because the number of such fractures is very small in comparison with the global number of cracks.

Cluster C (or (C + F) in M–S) contains relatively short signals with short rise time and low amplitude when compared to the others. Its activity during initial loading (Fig. 3) suggests that it corresponds to the last type of matrix cracking in M–E: C3-cracks in the axial yarns. These are the shortest cracks. Moreover, a saturation of the activity of this cluster is observed in M–E but not in M–S (Fig. 3a). This is in agreement with the fact that the multiple cracking saturation in the axial yarns is reached in M–E but not in M–S, due to the difference in the interface characteristics [1]. This has been confirmed by the microscopic observations. From the average crack spacing of 0.33 mm, 25 000 cracks are estimated in M–E, associated with only 3600 AE events (Table 1). In M–S, nearly 12 000 signals of cluster (C + F) have been recorded whereas 150 000 cracks are likely to be created in this material. This large discrepancy is probably due to the high acquisition threshold level (40 dB). The C-type signals have a low energy and some of them may not be detected because of their too low amplitudes.

Cluster D: this cluster is the last one to be activated, and it becomes more active as strain increases (Fig. 3). D-type signals seem to be a consequence of the existing damage in the material, and are more likely attributed to fibre–matrix interfacial debonding (C4-cracks). The D-type signals have the particularity of having a longer rise time than the other ones (Table 2), therefore the shapes of these signals are well differentiated from the others. This mechanism is especially expected to occur during the load hold sequence; this is actually the case for cluster D. As for C-type signals, some D-type signals were probably not recorded because of their low level of amplitude.

Cluster E only appears in M–S composite. The only additional observed mechanism in that material is the dense C5-cracking in a particular matrix layer of M–S. The energy of the corresponding signals is expected to be smaller than the A-type signals but larger than the C-type signals; this is the case of the cluster E (Table 1). The number of signals is consistent with the estimated number of cracks.

7. Conclusion

As a conclusion, a scenario for the identification of each cluster with one ore more damage mechanisms has been achieved taking into account the differences between the two studied composites. In the first paper [1] we analysed the different mechanical behaviours in relation with microscopic observations of the damage states after tensile tests. It has been shown that the global AE activity is different in both composites, which is in agreement with different damage accumulation scenarios. In this second paper, the AE data was subjected to an unsupervised multi-variate clustering analysis, which allows revealing the natural structure of the data. It has been pointed out that several types of signals can be distinguished, and that the obtained clusters are coherent with the expected differentiation of damage mechanisms. In particular, the different kinds of matrix cracking occurring in 3D-composites are well distinguished by the algorithm. The numbers of signals are in agreement with the rough estimations of the associated numbers of cracks, except for the low energy signals because the acquisition threshold value is too high to detect

all of them. The signals corresponding to fibre failures were not separated by the algorithm, probably because of the small number of related signals.

This methodology will further be applied to static fatigue experiments monitored by AE at intermediate temperatures on a SiC_f/[Si–B–C] composite. Clustering of AE data should be helpful to monitor the different damage kinetics and to perform reliable predictions of lifetimes.

Acknowledgements

The authors gratefully acknowledge Snecma Propulsion Solide, CNRS and DGA for supporting this work in the frame of the CPR: 'Modélisation, extrapolation, validation de la durée de vie des CMC'.

References

[1] Moevus M, Rouby D, Godin N, R'Mili M, Reynaud P, Fantozzi G, et al. Analysis of damage mechanisms and associated acoustic emission in two SiC/[Si–B–C] composites exhibiting different tensile curves. Part I: Damage patterns and acoustic emission activity. Compos Sci Technol 2008;68(6):1250–7.
[2] Beattie AG. Acoustic emission, principles and instrumentation. J Acoust Emission 1983;2(1/2):95–128.
[3] Eitzen DG, Wadley NG. Acoustic emission: establishing the fundamentals. J Res Nat Bur Stand 1984;89(1):75–100.
[4] Pollock AA. Acoustic emission amplitudes. NDT 1973:264–9.
[5] Shiwa M, Chen OY, Kishi T, Carpenter S, Mitsuno S, Ichikawa H, et al. Fracture mechanisms in unnotched and notched SiC/SiC composites studied by acoustic emission analysis. Mater Trans 1995;36(4):511–7.
[6] Surgeon M, Vanswijgenhoven E, Wevers M, Van Der Biest O. Acoustic emission during tensile testing of SiC-fibre-reinforced BMAS glass-ceramic composites. Compos Part A 1997;28A:473–80.
[7] Kaya F. Damage assessment of oxide fibre reinforced oxide ceramic matrix composites using acoustic emission. Ceram Int 2007;33:279–84.
[8] Morscher GN, Martinez-Fernandez J, Purdy MJ. Determination of interfacial properties using a single-fiber microcomposite test. J Am Ceram Soc 1996;79(4):1083–91.
[9] Morscher GN, Martinez-Fernandez J. Fiber effects on minicomposite mechanical properties for several silicon carbide fiber-chemically vapour-infiltrated silicon carbide matrix systems. J Am Ceram Soc 1999;82(1):145–55.
[10] Anastassopoulos AA, Philippidis TP. Clustering methodology for the evaluation of AE from composites. J Acoust Emission 1995;13(1/2):11–22.
[11] Anastassopoulos AA, Philippidis TP, Paipetis SA. Failure mechanism identification in composite materials by means of acoustic emission: Is it possible? In: Van Hemelrijck, Anastassopoulos, editors. Non Destructive Testing. Rotterdam: A.A. Balkema; 1996. p. 143–9.
[12] Pappas YZ, Markopoulos YP, Kostopoulos V. Failure mechanisms analysis of 2D carbon/carbon using acoustic emission monitoring. NDT&E Int 1998;31(3):157–63.
[13] Kostopoulos V, Loutas TH, Kontsos A, Sotiriadis G, Pappas YZ. On the identification of the failure mechanisms in oxide/oxide composites using acoustic emission. NDT&E Int 2003;36:571–80.
[14] Kostopoulos V, Loutas T, Dassios K. Fracture behavior and damage mechanisms identification of SiC/glass ceramic composites using AE monitoring. Compos Sci Technol 2007;67:1740–6.
[15] Huguet S, Godin N, Gaertner R, Salmon L, Villard D. Use of acoustic emission to identify damage modes in glass fibre reinforced polyester. Compos Sci Technol 2002;62:1433–44.
[16] Godin N, Huguet S, Gaertner R, Salmon L. Clustering of acoustic emission signals collected during tensile tests on unidirectional glass/polyester composite using supervised and unsupervised classifiers. NDT&E Int 2004;37:253–64.
[17] Godin N, Huguet S, Gaertner R. Integration of the Kohonen's self-organising map and *k*-means algorithm for the segmentation of the AE data collected during tensile tests on cross-ply composites. NDT&E Int 2005;38(4):299–309.
[18] Johnson M. Waveform based clustering and classification of AE transients in composite laminates using principal component analysis. NDT&E Int 2002;35:367–76.
[19] Morscher GN. Modal acoustic emission of damage accumulation in a woven SiC/SiC composite. Compos Sci Technol 1999;59:687–97.
[20] Morscher GN. Stress dependent matrix cracking in 2D woven SiC-fibre reinforced melt-infiltrated SiC matrix composites. Compos Sci Technol 2004;64:1311–9.
[21] Pappas YZ, Kontsos A, Loutas TH, Kostopoulos V. On the characterization of continuous fibres fracture by quantifying acoustic emission and acousto-ultrasonics waveforms. NDT&E Int 2004;37:389–401.
[22] Loutas TH, Kostopoulos V, Ramirez-Jimenez C, Pharaoh M. Damage evolution in center-holed glass/polyester composites under quasi-static loading using time/frequency analysis of acoustic emission monitored waveforms. Compos Sci Technol 2006;66:1366–75.
[23] Moevus M, Reynaud P, R'Mili M, Godin N, Rouby D, Fantozzi G. Static fatigue of a 2.5D SiC/[Si–B–C] composite at intermediate temperature under air. Adv Sci Technol 2006;50:141–6.
[24] Jain AK, Murty MN, Flynn PJ. Data clustering: a review. ACM Comput Surveys 1999;31(3):264–323.
[25] Jain AK, Duin RPW, Mao J. Statistical pattern recognition: a review. IEEE Trans Pattern Anal Mach Intell 2000.
[26] Anderberg MR. Cluster analysis for applications. Academic Press; 1973.
[27] Saporta G. Probabilités, analyse de données et statistique. Ed Technip; 1990.
[28] Ding C, He X. *K*-means clustering via principal component analysis. In: Proceedings of the 21st international conference on machine learning, Banff, Canada; 2004.
[29] MacQueen J. Some methods for classification and analysis of multivariate observations. In: LeCam LM, Neyman J, editors. Proceedings of the 5th Berkeley symposium on mathematical statistics and probability. University of California Press; 1967. p. 281–97.
[30] Davies AL, Bouldin DW. A cluster separation measure. IEEE Trans Pattern Anal Mach Intell 1979;PAMI-1:224–7.